ANL/EVS/R-12/2

Soil Carbon Response to Rising Temperature

Environmental Science Division

About Argonne National Laboratory

Argonne is a U.S. Department of Energy laboratory managed by UChicago Argonne, LLC under contract DE-AC02-06CH11357. The Laboratory's main facility is outside Chicago, at 9700 South Cass Avenue, Argonne, Illinois 60439. For information about Argonne and its pioneering science and technology programs, see www.anl.gov.

Availability of This Report

This report is available, at no cost, at http://www.osti.gov/bridge. It is also available on paper to the U.S. Department of Energy and its contractors, for a processing fee, from:

U.S. Department of Energy
Office of Scientific and Technical Information
P.O. Box 62
Oak Ridge, TN 37831-0062
phone (865) 576-8401
fax (865) 576-5728
reports@adonis.osti.gov

Disclaimer

This report was prepared as an account of work sponsored by an agency of the United States Government. Neither the United States Government nor any agency thereof, nor UChicago Argonne, LLC, nor any of their employees or officers, makes any warranty, express or implied, or assumes any legal liability or responsibility for the accuracy, completeness, or usefulness of any information, apparatus, product, or process disclosed, or represents that its use would not infringe privately owned rights. Reference herein to any specific commercial product, process, or service by trade name, trademark, manufacturer, or otherwise, does not necessarily constitute or imply its endorsement, recommendation, or favoring by the United States Government or any agency thereof. The views and opinions of document authors expressed herein do not necessarily state or reflect those of the United States Government or any agency thereof, Argonne National Laboratory, or UChicago Argonne, LLC.

ANL/EVS/R-12/2

Soil Carbon Response to Rising Temperature

prepared by
A. Montz,[1,2] V. R. Kotamarthi,[1] and H. Bellout[2]
[1]Argonne National Laboratory
[2]Northern Illinois University

July 2012

Work supported by the U.S. Department of Energy, Office of Science,
Office of Biological and Environmental Research.

Contents

Notation . . . . . **iii**

Objective and Overview **1**

Analysis Methodology and Results **3**

Conclusion **16**

References **17**

List of Tables

1 Constant values for the linear model (1) used in [9]. 18
2 Parameter values for the nonlinear model (6). 18

List of Figures

1 Projections of the phase space to the planes M_1M_2, M_2M_3, and M_3M_4, respectively. 7
2 Plots of $b_1(t), b_2(t), b_3(t)$, and $b_4(t)$ and their equilibrium values, respectively. 8
3 Plots of $M_1(t), M_2(t), M_3(t)$, and $M_4(t)$ and their equilibrium values, respectively. 8
4 NCE over the temperature range 288 K $\leq T \leq$ 298 K 9
5 NCE over a range of the Arrhenius constant A. 11
6 NCE over a range of the constant c_1. 11
7 NCE over a range of the constant c_2. 12
8 NCE over a range of the microbial activation energy E_{am}. . . . 12
9 NCE over a range of the physico-chemical activation energy E_{ap}. 13
10 NCE over a range of the substrate concentration constant G. . 13
11 NCE over a range of the maximum percentage of biomass in each pool p. 14
12 NCE over a range of the net primary production P_n. 14
13 NCE over the temperature range 288 K $\leq T \leq$ 298 K, with P_n a linear function of T. 15

Notation

C	carbon
cm	centimeter(s)
d	day(s)
h	hour(s)
K	degree(s) Kelvin
kg	kilogram(s)
kJ	kilojoule(s)
m	meter(s)
mg	milligram(s)
mol	mole
NCE	net carbon at equilibrium
T	temperature

Objective and Overview

The primary objective of this study was to investigate soil carbon response to rising temperatures by generalizing a linear four-pool soil carbon model introduced by Thornley and Cannell [9]. Currently, all of the major models predict that soil respiration will increase more than net primary productivity, P_n, as temperatures rise [9]. However, some have questioned these predictions, pointing to a lack of evidence of decreasing soil carbon in some parts of the world as annual mean temperatures have risen. The current explanation for this contradiction is that soil respiration's temperature sensitivity has been overestimated in the models. However, the soil respiration data are conflicting, making this explanation unsatisfactory [9].

Thornley and Cannell [9] propose an alternative explanation. They hypothesize that warming increases the rate of physico-chemical processes that transfer soil carbon to stable, protected pools, as opposed to releasing it into the atmosphere. These physico-chemical processes in turn respond more to warming than does microbial respiration, which is responsible for soil respiration. To study this hypothesis, the authors created the linear model of four soil carbon pools given by Figure 3 in [9].

Carbon pools M_1, M_2, and M_3 have fast, intermediate, and slow turnover times, respectively. Pool M_4 is the protected, stabilized pool. The system has one input, P_n, into pool M_1. Transfers between pools are denoted by the rate constants k_{ij}. Transfers denoted with a solid line, $k_{ij}, i \neq 4$ or $j \neq 4$, are due to microbial processes. Half of the carbon transferred is lost from the system. Microbial processes also cause a direct loss from each pool, denoted by $k_i, 1 \leq i \leq 4$. Transfers denoted with a dashed line, $k_{ij}, i = 4$ or $j = 4$, are due to physico-chemical process.

The governing equations of this system are as follows:

$$\frac{dM_1}{dt} = P_n + \frac{1}{2}k_{21}M_2 + \frac{1}{2}k_{31}M_3 + k_{41}M_4 - (k_1 + k_{12} + k_{13} + k_{14})\, M_1 \quad \text{(1a)}$$

$$\frac{dM_2}{dt} = \frac{1}{2}k_{12}M_1 + \frac{1}{2}k_{32}M_3 + k_{42}M_4 - (k_{21} + k_2 + k_{23} + k_{24})\, M_2 \quad \text{(1b)}$$

$$\frac{dM_3}{dt} = \frac{1}{2}k_{13}M_1 + \frac{1}{2}k_{23}M_2 + k_{43}M_4 - (k_{31} + k_{32} + k_3 + k_{34})\, M_3 \quad \text{(1c)}$$

$$\frac{dM_4}{dt} = \frac{1}{2}k_{14}M_1 + \frac{1}{2}k_{24}M_2 + k_{34}M_3 - (k_{41} + k_{42} + k_{43} + k_4)\, M_4 \quad \text{(1d)}$$

Values of the rate constants are chosen to conform to the supposed turnover time of each pool (see Table 1).

The system is assumed to have one stable equilibrium point. (This can easily be proven.) Denote $M_i(\infty) = \lim_{t\to\infty} M_i$ and $M_\infty = M_1(\infty) + M_2(\infty) + M_3(\infty) + M_4(\infty)$. For the chosen values of the constants, $M_\infty = 13.3\ \mathrm{kg\,C\,m^{-2}}$.

The goal in studying the system (1a)-(1d) is to understand how the net carbon at equilibrium (NCE) changes with temperature. Note that the temperature, T, does not occur explicitly in the system. To simulate a rise in temperatures in [9], P_n is increased by a factor of 1.3, and all rate constants are increased by a factor of 1.5. The physico-chemical rate constants are then further increased by factors of $2.25, 3, 3.75$, and 4 to simulate their greater sensitivity to temperature. An increase in the physico-chemical processes relative to the microbial is shown to cause the NCE to increase.

These results are not supported by experimental evidence. However, this model (1) exhibits the hypothesis that warming may transfer carbon to a more stable, protected pool. This results in no loss of NCE with rising temperatures, without ignoring the temperature sensitivity of microbial respiration.

In this report we expand upon the linear model (1) by adding modeling assumptions to each type of reaction, physico-chemical and microbial, and add a population model for the microbial biomass in each pool. This results in a nonlinear model in which the temperature, T, appears explicitly. We first

show that this model has a unique, positive, and stable equilibrium point, and then proceed to study how the NCE changes as we vary the temperature parameter. Furthermore, our model has numerous other parameters, and we study how the NCE changes as we vary each of these parameters.

For further work on the temperature sensitivity of soil carbon and its role in feedbacks to climate change, see [1], [2], [3], [4], and [10]. Mathematical models to study this problem have been developed in [5] and [6].

Analysis Methodology and Results

Denote the amount of carbon and microbial biomass in the ith pool by $M_i(t;T)$ and $b_i(t;T)$, respectively.

To model the microbial biomass in each pool, we use the logistic model of population growth

$$\frac{db_i}{dt} = r_i b_i \left(1 - \frac{b_i}{b_{max}}\right) , \tag{2}$$

where r_i and b_{max} are the growth rate and carrying capacity of the ith pool, respectively. The growth rate must depend on the carbon available (for a study of this assumption, see [8]). We assume that

$$r_i = \frac{M_i}{1 + M_i} . \tag{3}$$

Also, assume that b_i can reach a maximum percent, $0 < p_i < 1$, of M_i:

$$b_{max} = p_i M_i \tag{4}$$

Rate constants k_{ij}, $i = 4$ or $j = 4$ are physico-chemical. They will be modeled with the Arrhenius equations, $k_{ij} = Ae^{-E_{ap}/RT}$, where A is the Arrhenius constant, E_{ap} is the activation energy for physico-chemical reactions, R is the gas constant, and T is temperature.

Rate constants k_i, $1 \leq i \leq 4$ and k_{ij}, $1 \leq i, j \leq 3$ are microbial and will be modeled with Michaelis-Menten kinetics. Let the enzyme substrate concentration be S. Then $S_i = Gb_i$, where G is a constant substrate concentration.

If we assume that all microbes in all pools are similar, then $k_{ij} = \frac{V_{max} S_i}{K+S_i}$. Furthermore, assume that V_{max} is governed by the Arrhenius equation (as in [1]), $V_{max} = Ae^{-E_{am}/RT}$, where E_{am} is the activation energy for microbial reactions. Assume that $E_{am} < E_{ap}$, so that the physico-chemical reactions have greater temperature sensitivity, which is the hypothesis in [9]. Also assume that K depends linearly on temperature; i.e. $K = c_1 T + c_2$ [1].

Thus, we have the following:

$$\begin{cases} k_{ij} = Ae^{-E_{ap}/RT} & i = 4 \text{ or } j = 4 \\ k_{ij} = \dfrac{Ae^{-E_{am}/RT} Gb_i}{c_1 T + c_2 + Gb_i} & 1 \leq i, j \leq 3 \\ k_i = \dfrac{Ae^{-E_{am}/RT} Gb_i}{c_1 T + c_2 + Gb_i} & 1 \leq i \leq 4 \end{cases} \tag{5}$$

Inserting the assumption (5) into (1) and assumptions (3) and (4) into (2) results in the following system of eight ordinary differential equations for the microbial biomass and carbon of each pool:

$$\frac{db_1}{dt} = \frac{M_1 b_1}{1 + M_1} \left(1 - \frac{b_1}{p_1 M_1}\right) \tag{6a}$$

$$\frac{db_2}{dt} = \frac{M_2 b_2}{1 + M_2} \left(1 - \frac{b_2}{p_2 M_2}\right) \tag{6b}$$

$$\frac{db_3}{dt} = \frac{M_3 b_3}{1 + M_3} \left(1 - \frac{b_3}{p_3 M_3}\right) \tag{6c}$$

$$\frac{db_4}{dt} = \frac{M_4 b_3}{1 + M_4} \left(1 - \frac{b_4}{p_4 M_4}\right) \tag{6d}$$

$$\begin{aligned} \frac{dM_1}{dt} &= P_n + Ae^{-E_{ap}/RT} (M_4 - M_1) + \\ &\frac{1}{2} GAe^{-E_{am}/RT} \left(\frac{-6b_1 M_1}{c_1 T + c_2 + Gb_1} + \frac{b_2 M_2}{c_1 T + c_2 + Gb_2} + \frac{b_3 M_3}{c_1 T + c_2 + Gb_3} \right) \end{aligned} \tag{6e}$$

$$\frac{dM_2}{dt} = Ae^{-E_{ap}/RT}\left(M_4 - M_2\right) + \tag{6f}$$
$$\frac{1}{2}GAe^{-E_{am}/RT}\left(\frac{b_1M_1}{c_1T + c_2 + Gb_1} - \frac{6b_2M_2}{c_1T + c_2 + Gb_2} + \frac{b_3M_3}{c_1T + c_2 + Gb_3}\right)$$

$$\frac{dM_3}{dt} = Ae^{-E_{ap}/RT}\left(M_4 - M_3\right) + \tag{6g}$$
$$\frac{1}{2}GAe^{-E_{am}/RT}\left(\frac{b_1M_1}{c_1T + c_2 + Gb_1} + \frac{b_2M_2}{c_1T + c_2 + Gb_2} - \frac{6b_3M_3}{c_1T + c_2 + Gb_3}\right)$$

$$\frac{dM_4}{dt} = Ae^{-E_{ap}/RT}\left(M_1 + M_2 + M_3 - 3M_4\right) - \frac{GAe^{-E_{am}/RT}b_4M_4}{c_1T + c_2 + Gb_4}. \tag{6h}$$

Standard values for the parameters in (6) are given in Table 2.

We are interested in the effect of temperature on the NCE. Therefore, we first show that the system has one positive, stable equilibrium point for the standard parameter values.

Denote the equilibrium point by (b_i^*, M_i^*). We require that $b_i^*, M_i^* > 0$. In equations (6a)-(6d)

$$\frac{db_i}{dt} = 0 \Leftrightarrow b_i = 0, M_i = 0 \text{ or } b_i = p_iM_i\,. \tag{7}$$

So

$$b_i^* = p_iM_i^*\,. \tag{8}$$

We can insert (8) into (6e)-(6h) at equilibrium, which gives the following

$$F_1(M_1, M_2, M_3, M_4; T) \equiv P_n + Ae^{-E_{ap}/RT}\left(M_4^* - M_1^*\right) \tag{9}$$
$$+ \frac{1}{2}GpAe^{-E_{am}/RT}\left(\frac{-6(M_1^*)^2}{c_1T + c_2 + GpM_1^*} + \frac{(M_2^*)^2}{c_1T + c_2 + GpM_2^*} + \frac{(M_3^*)^2}{c_1T + c_2 + GpM_3^*}\right)$$
$$= 0$$

$$F_2(M_1, M_2, M_3, M_4; T) \equiv Ae^{-E_{ap}/RT}\,(M_4^* - M_2^*) \tag{10}$$

$$+\frac{1}{2}GpAe^{-E_{am}/RT}\left(\frac{(M_1^*)^2}{c_1T + c_2 + GpM_1^*} - \frac{6(M_2^*)^2}{c_1T + c_2 + GpM_2^*} + \frac{(M_3^*)^2}{c_1T + c_2 + GpM_3^*}\right)$$

$$= 0$$

$$F_3(M_1, M_2, M_3, M_4; T) \equiv Ae^{-E_{ap}/RT}\,(M_4^* - M_3^*) \tag{11}$$

$$+\frac{1}{2}GpAe^{-E_{am}/RT}\left(\frac{(M_1^*)^2}{c_1T + c_2 + GpM_1^*} + \frac{(M_2^*)^2}{c_1T + c_2 + GpM_2^*} - \frac{6p(M_3^*)^2}{c_1T + c_2 + GpM_3^*}\right)$$

$$= 0$$

$$F_4(M_1, M_2, M_3, M_4; T) \equiv \tag{12}$$

$$Ae^{-E_{ap}/RT}\,(M_1^* + M_2^* + M_3^* - 3M_4^*) - \frac{GpAe^{-E_{am}/RT}(M_4^*)^2}{c_1T + c_2 + GpM_4^*} = 0.$$

Mathematica is used to solve equations (9)-(12) for the four unknowns $(M_1^*, M_2^*, M_3^*, M_4^*)$ with the parameter values from Table 2. There is one positive equilibrium point:

$$(M_1^*, M_2^*, M_3^*, M_4^*) = (12.80, 12.32, 12.32, 12.46)\,\mathrm{mg\,C\,cm^{-2}} \tag{13}$$

Substituting (13) into (8) gives the biomass equilibrium, which is

$$(b_1^*, b_2^*, b_3^*, b_4^*) = (0.64, 0.62, 0.62, 0.62)\,\mathrm{mg\,biomass\,cm^{-2}}\,. \tag{14}$$

Linearizing the system (6) about the equilibrium point given by (13) and (14) and computing the eigenvalues, λ_i, of the resulting Jacobian gives the following values:

$$\lambda_1 = -1.30 \quad \lambda_2 = -1.30 \quad \lambda_3 = -1.29 \quad \lambda_4 = -1.25$$

$$\lambda_5 = -0.51 \quad \lambda_6 = -0.43 \quad \lambda_7 = -0.43 \quad \lambda_8 = -0.04$$

Since the equilibrium point is hyperbolic (i.e. $\lambda_i \neq 0, \forall i$), the Hartman-Grobman theorem [7] applies. Therefore, the equilibrium point is stable, because $Re(\lambda_i) < 0, \forall i$.

The stability of the equilibrium point can be seen in the phase space. We cannot plot the phase space, as it is 8-dimensional, but we can plot projections in various planes (see Figure 1).

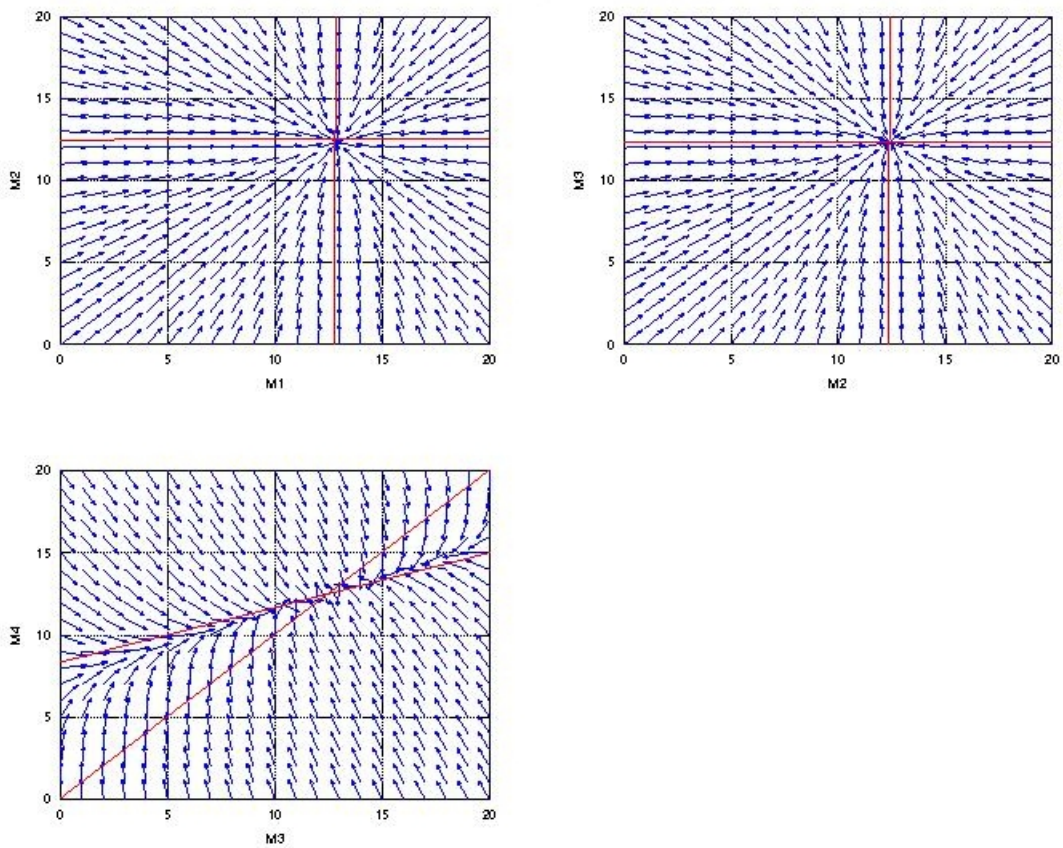

FIGURE 1: Projections of the phase space to the planes M_1M_2, M_2M_3, and M_3M_4, respectively. The M_i not shown are set to their equilibrium values. Red lines indicate where $\frac{dM_i}{dt} = 0$, and their intersection is the equilibrium point.

The stability of the equilibrium point can also be seen in plots of the solution to (6) in time (see Figures 2 and 3), which show that $(b_i(t), M_i(t)) \to (b_i^*(t), M_i^*(t))$ as $t \to \infty$.

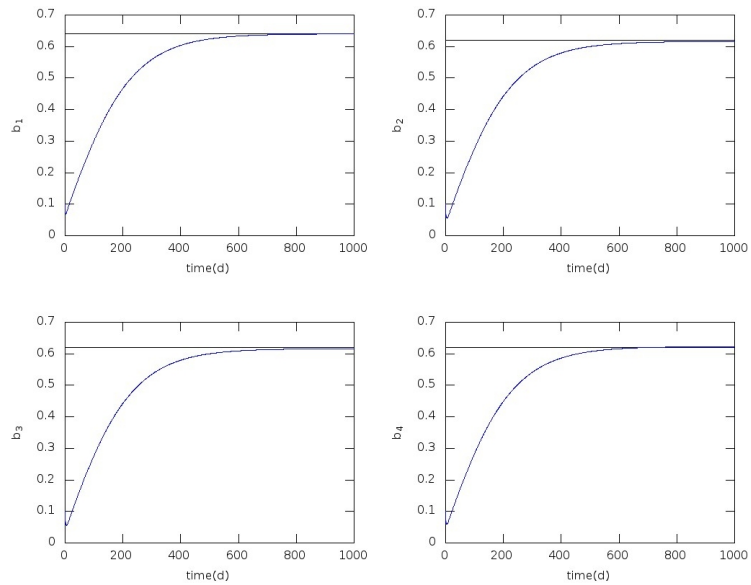

FIGURE 2: Plots of $b_1(t), b_2(t), b_3(t)$, and $b_4(t)$ and their equilibrium values, respectively. Each solution approaches equilibrium (the black line) as $t \to \infty$.

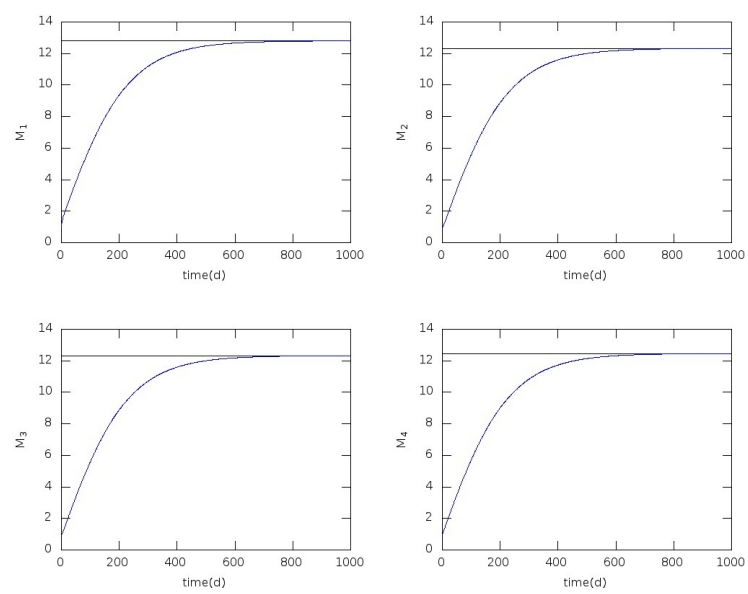

FIGURE 3: Plots of $M_1(t), M_2(t), M_3(t)$, and $M_4(t)$ and their equilibrium values, respectively. Each solution approaches equilibrium (the black line) as $t \to \infty$.

Now that we have one positive, stable equilibrium point, our goal is to study how this equilibrium point changes with temperature.

As temperature, T, is an explicit parameter of the system (6), we calculate the equilibrium point, as was done above, over the range of temperatures 288 K $\leq T \leq$ 298 K and plot the NCE, $M_1^* + M_2^* + M_3^* + M_4^*$, over this range (see Figure 4). Note that for each T in this range, there is one positive, stable equilibrium point.

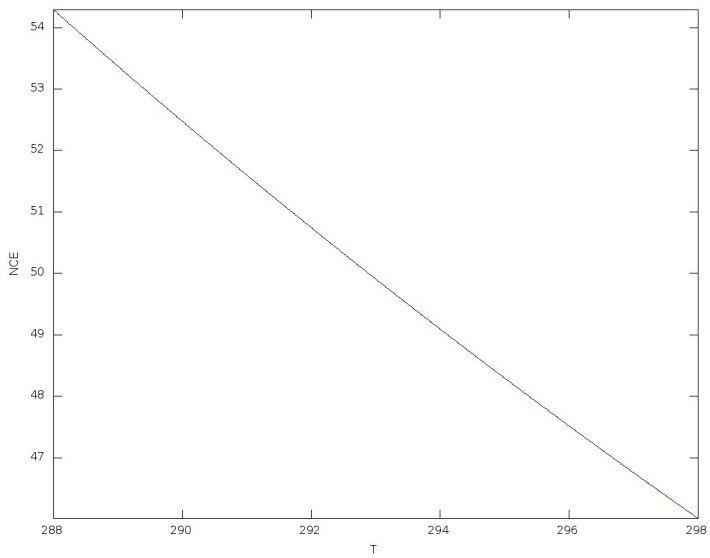

FIGURE 4: NCE over the temperature range 288 K $\leq T \leq$ 298 K

We now prove formally that the NCE is decreasing with increasing temperature, as can be seen in Figure 4.

Proposition. *At the base temperature of* $T = 293$ K*, NCE is decreasing with increasing temperature.*

Proof. Differentiating (9)-(12) with respect to T gives, for each $1 \leq i \leq 4$,

$$0 = \frac{\partial[F_i(M_j^*(T), T)]}{\partial T} = \frac{\partial F_i}{\partial T} + \sum_{j=1}^{4} \frac{\partial F_i}{\partial M_j^*} \frac{\partial M_j^*}{\partial T} \tag{15}$$

Solving (15) for $\dfrac{\partial M_j^*}{\partial T}$ and writing the result in vector notation gives

$$\frac{\partial \mathbf{M}^*}{\partial T} = -[\nabla \mathbf{F}]^{-1} \frac{\partial \mathbf{F}}{\partial T}\,, \tag{16}$$

where $\mathbf{M}^* = (M_1^*, M_2^*, M_3^*, M_4^*)^T$ and $\nabla \mathbf{F} = \dfrac{\partial F_i}{\partial M_j}$. For $T = 293$ K we calculate that

$$\left.\frac{\partial \mathbf{M}^*}{\partial T}\right|_{T=293} = (-0.81, -0.79, -0.79, -0.63)^T \tag{17}$$

Thus, NCE is decreasing with increasing T. □

The decreasing NCE with a rise in temperature for the nonlinear model (6) is in contrast to the results for the linear model (1) as found in [9].

The system (6) contains numerous parameters (see Table 2). Some are not readily found in the literature, and some are difficult to estimate [1]. However, the qualitative behavior of the system does not depend upon the specific values of the parameters. In Figures 5-12, we plot the NCE over a range of values for each parameter. In each case, there is a positive, stable equilibrium point.

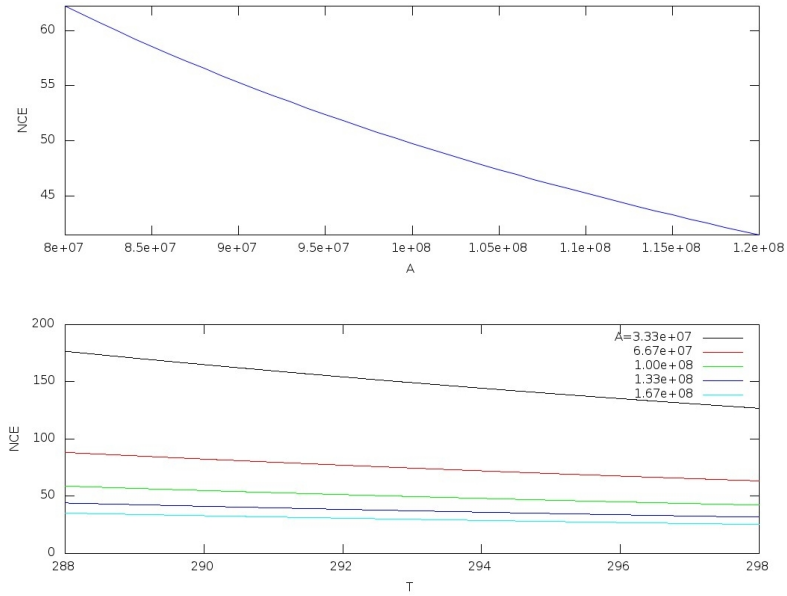

FIGURE 5: NCE over a range of the Arrhenius constant A.

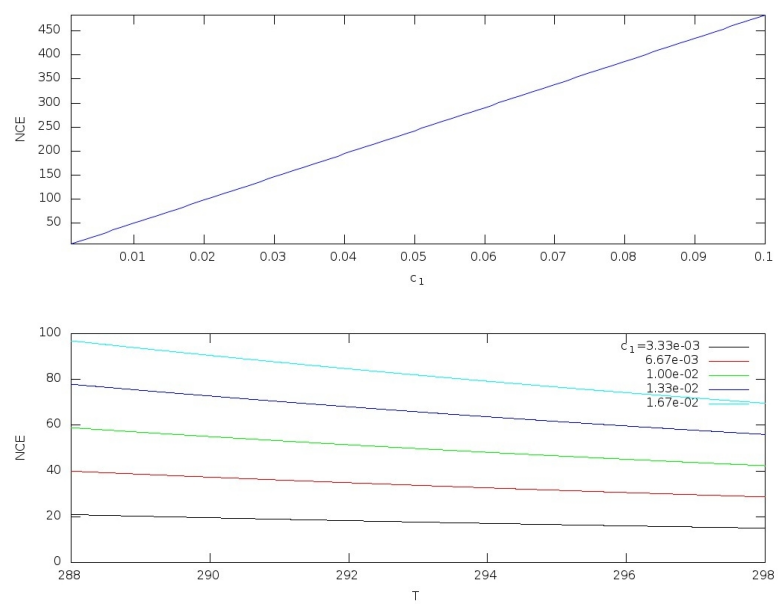

FIGURE 6: NCE over a range of the constant c_1.

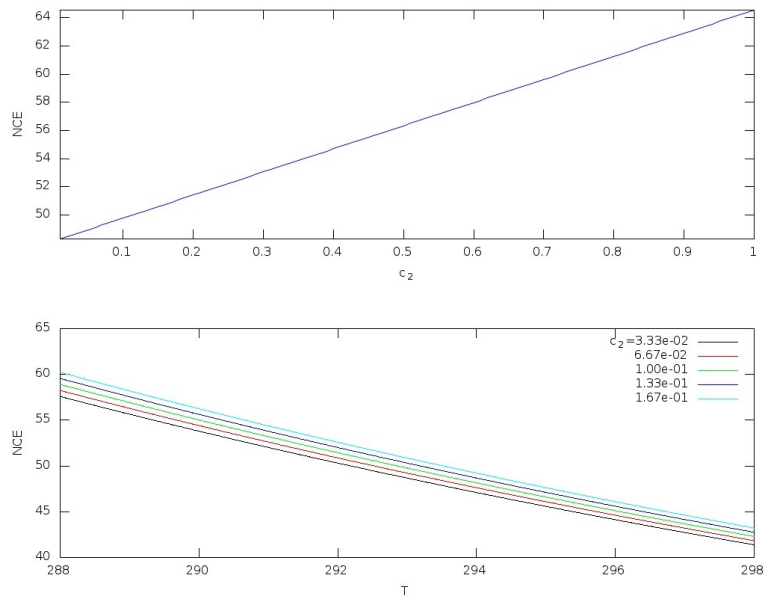

FIGURE 7: NCE over a range of the constant c_2.

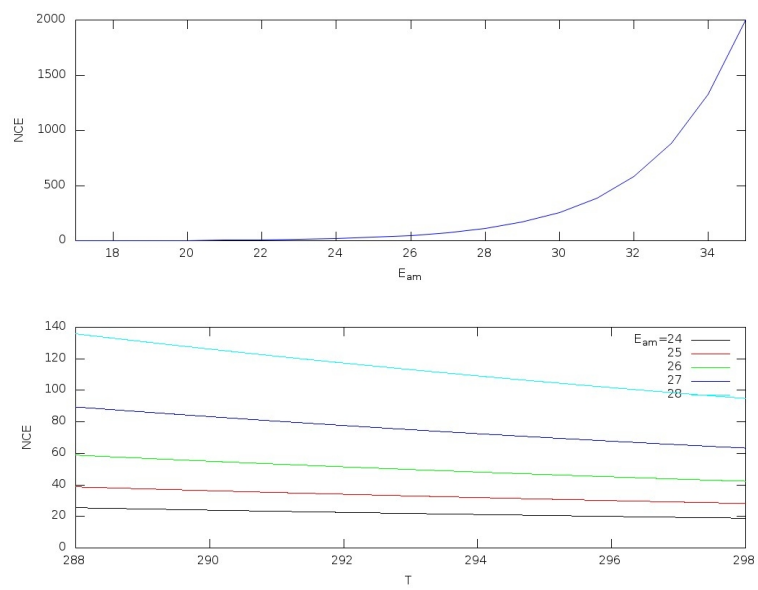

FIGURE 8: NCE over a range of the microbial activation energy E_{am}.

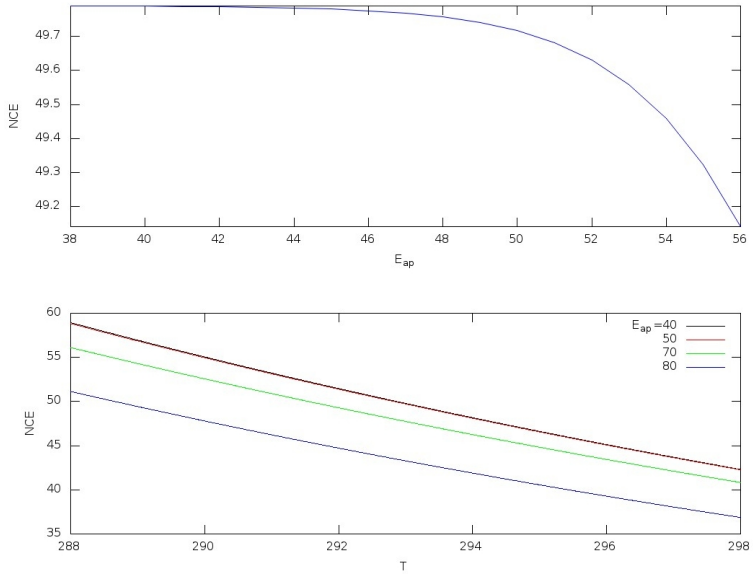

FIGURE 9: NCE over a range of the physico-chemical activation energy E_{ap}.

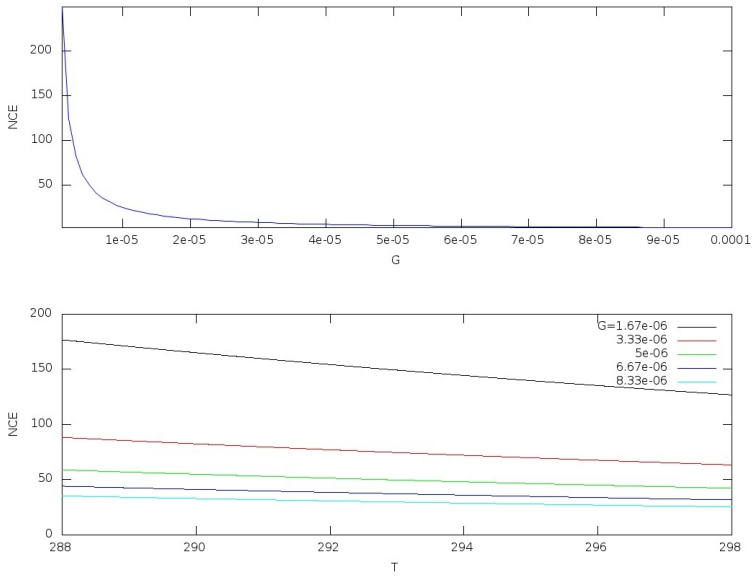

FIGURE 10: NCE over a range of the substrate concentration constant G.

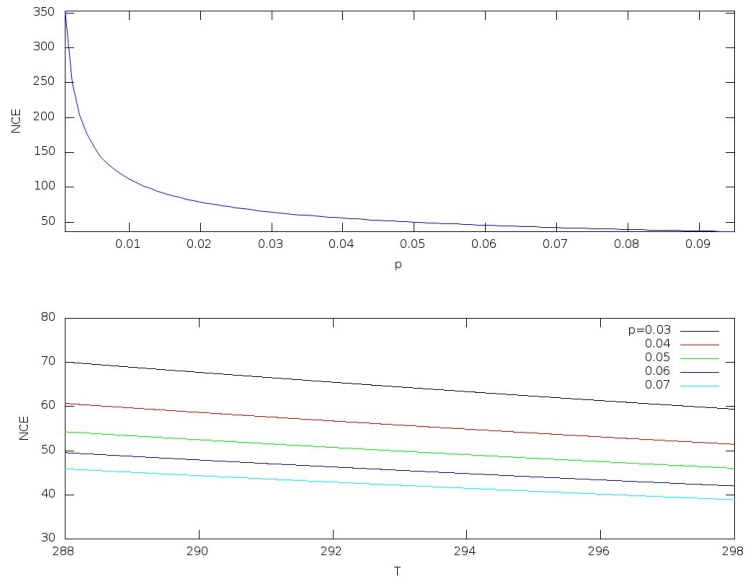

FIGURE 11: NCE over a range of the maximum percentage of biomass in each pool p.

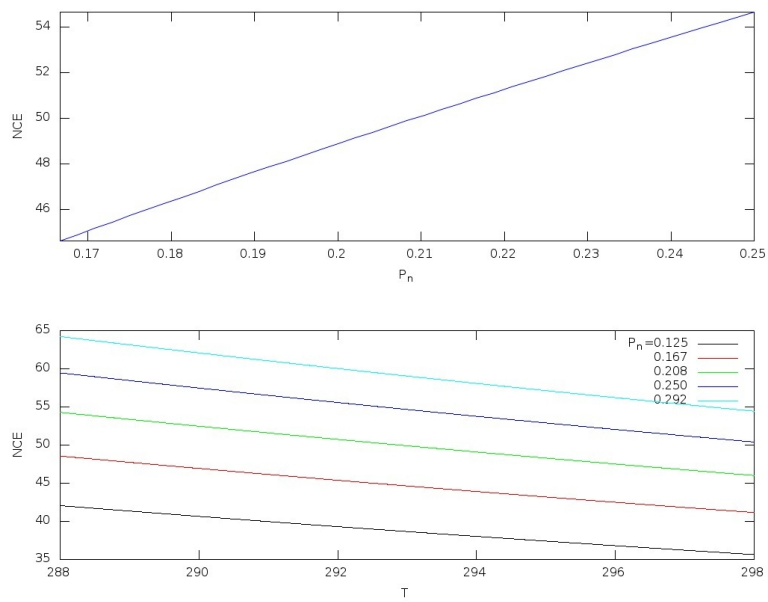

FIGURE 12: NCE over a range of the net primary production P_n.

In [9], the authors assume that net primary productivity, P_n, rises with temperature; in fact, the authors increase this constant by a factor of 1.3 to simulate such a rise. Also, Figure 12, shows that NCE rises with increasing P_n. This is expected, because P_n is the sole input of carbon into the system. For these reasons, it is reasonable to assume that NCE will increase with temperature if P_n does as well.

Let us now assume that P_n depends linearly on temperature and take

$$P_n(T) = 0.01(T - 293) + \frac{5}{24}\,, \tag{18}$$

where $T = 293$ K and $P_n = \dfrac{5}{24}$ mg C cm^{-3} h^{-1} are the base values for temperature and net primary productivity, respectively. The equilibrium point is unchanged for $T = 293$ K (see (15)). Recomputing (16), the rate of change of the carbon in each pool with temperature, at $T = 293$ K, we now find that

$$\left.\frac{\partial \mathbf{M}^*}{\partial T}\right|_{T=293} = (0.087, 0.096, 0.096, 0.093)^T\,. \tag{19}$$

With this small change to P_n, the NCE now rises with increasing temperature, as can be seen in Figure 13, consistent with [9].

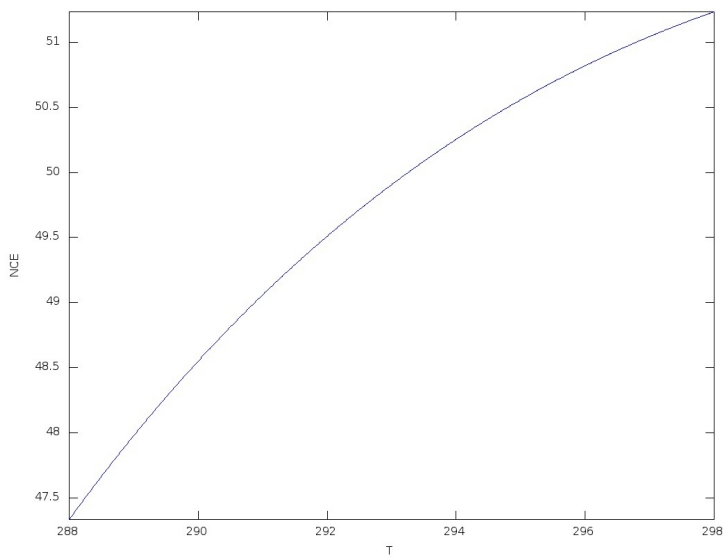

FIGURE 13: NCE over the temperature range 288 K $\leq T \leq$ 298 K, with P_n a linear function of T.

Conclusion

Currently, models predict a decrease in soil carbon stocks with rising temperatures. This conclusion is questioned, because it does not agree with empirical evidence. In [9], the authors propose a hypothesis to resolve this discrepancy in support of the empirical evidence and create a model to study their hypothesis.

In this report, we expand the model of Thornley and Cannell [9] by modeling each implicit assumption and making temperature an explicit parameter. This allows us to study directly the system's behavior over a range of temperatures. Making these assumptions, however, introduces many other parameters (see Table 2), some of which are difficult to estimate. For our chosen parameter values, we found a positive, stable equilibrium point and showed that NCE decreased with increasing temperature for constant net primary productivity. When we assumed a small linear increase in net primary productivity, the behavior changed; NCE rose with temperature. This observation might illustrate why studies arrive at conflicting results. A small change in parameters can drastically change the behavior of the system.

References

[1] S. D. Allison, M. D. Wallenstein, and M. A. Bradford, *Soil-carbon response to warming dependent on microbial physiology*, Nature Geoscience, 3 (2010), pp. 336–340.

[2] E. A. Davidson and I. A. Janssens, *Temperature sensitivity of soil carbon decomposition and feedbacks to climate change*, Nature, 440 (2006), pp. 165–173.

[3] M. U. F. Kirschbaum, *Will changes in soil organic carbon act as a positive or negative feedback on global warming?*, Biogeochemistry, 48 (2000), pp. 21–51.

[4] W. Knorr, I. C. Prentice, J. I. House, and E. A. Holland, *Long-term sensitivity of soil carbon turnover to warming*, Nature, 433 (2005), pp. 298–301.

[5] S. Manzoni and A. Porporato, *A theoretical analysis of nonlinearities and feedbacks in soil carbon and nitrogen cycles*, Soil Biology and Biochemistry, 39 (2007), pp. 1542–1556.

[6] S. Manzoni, A. Porporato, P. D'Odorico, F. Laio, and I. Rodriguez-Iturbe, *Soil nutrient cycles as a nonlinear dynamical system* , Nonlinear Processes in Geophysics, 11 (2004), pp. 589–598.

[7] L. Perko, *Differential Equations and Dynamical Systems*, Texts in Applied Mathematics, Springer, 3 ed., 2001.

[8] J. P. Schimel and M. N. Weintraub, *The implications of exoenzyme activity on microbial carbon and nitrogen limitation in soil: a theoretical model*, Soil Biology and Biochemistry, 35 (2003), pp. 549–563.

[9] J. Thornley and M. Cannell, *Soil Carbon Storage Response to Temperature: an Hypothesis*, Annals of Botany, 87 (2001), pp. 591–598.

[10] M. von Lützow and I. Kögel-Knabner, *Temperature sensitivity of soil organic matter decomposition—what do we know?*, Biology and Fertility of Soils, 46 (2009), pp. 1–15.

TABLE 1 Constant values for the linear model (1) used in [9].

$P_n = 0.005\ \mathrm{C\,m^{-2}\,d^{-1}}$

$k_1 = 2$	$k_{12} = 1$	$k_{13} = 0.6$	$k_{14} = 0.002$
$k_2 = 0.2$	$k_{21} = 0.1$	$k_{23} = 0.6$	$k_{24} = 0.002$
$k_3 = 0.02$	$k_{31} = 0.06$	$k_{32} = 0.06$	$k_{34} = 0.002$
$k_4 = 0.02$	$k_{41} = 0.0002$	$k_{42} = 0.0002$	$k_{43} = 0.0002$
			$\times 10^{-3}\ \mathrm{d}^{-1}$

TABLE 2 Parameter values for the nonlinear model (6).

Parameter	Value	Units	Source
P_n	$\frac{5}{24}$	$\mathrm{mg\,C\,cm^{-3}\,h^{-1}}$	[9]
A	100000000	$\mathrm{mg\,C\,cm^{-3}\,h^{-1}}$	[1]
E_{ap}	47	$\mathrm{kJ\,mol^{-1}}$	[1]
E_{am}	26	$\mathrm{kJ\,mol^{-1}}$	-
R	0.008314	$\mathrm{kJ\,mol^{-1}\,K}$	[1]
T	293	K	[1]
G	0.000005	-	-
c_1	0.01	$\mathrm{mg\,cm^{-3}\,K^{-1}}$	[1]
c_2	0.1	$\mathrm{mg\,cm^{-3}}$	[1]
p_i	0.05	-	-

Environmental Science Division
Argonne National Laboratory
9700 South Cass Avenue, Bldg. 203
Argonne, IL 60439-4843

www.anl.gov

Argonne National Laboratory is a U.S. Department of Energy
laboratory managed by UChicago Argonne, LLC